

MCNP4C3-BASED SIMULATION OF A MEDICAL LINEAR ACCELERATOR

Siva R. Manoharan,^{*}
Redding Cancer Treatment Center,
Redding, CA.
manohar_sr@yahoo.com

L. Venkatanarayana[†]
Loma Linda University Medical Center,
Loma Linda, CA.

M. Chandrasekar[‡]
Department of Physics,
Jawaharlal Nehru Technological University,
Hyderabad, India

ABSTRACT

The general purpose MCNP4c3 code was employed to calculate the dosimetric characteristics of the photon beams of 6 and 15MV from a Varian Clinac 2100 C/D. The entire geometry, including the accelerator head and the water phantom, was simulated to calculate the dose profiles and the relative depth-dose distribution. The accuracy of the calculated results was examined by comparison with measured dose distributions by the radiation field analyzer in the water phantom. The simulated data and measured depth dose curves agreed to within 1% for the 6MV and within 2% for the 15MV photons. The profiles of the 6 and 15MV were within 2% for all the depths between the simulated and measured data. The field edge of the 15MV profile showed the influence of spot size.

KEYWORDS: MCNP, monte carlo, linac

1. INTRODUCTION

The Monte Carlo technique has been the predominant method to simulate radiation transport with an emphasis on transport of photons and electrons (Lovell et al., 1995). The increased use of the Monte Carlo technique is partially due to the increase in computing power within the last few years. This method of simulation involves two stages of work (Rogers, 2006): 1) linac head geometry simulation and 2) patient simulation.

Research has documented the use of the Los Alamos-developed Monte Carlo-N-particle (MCNP) radiation transport code for simulating particle transport and modeling the key components of a treatment head to acquire energy and spectral distributions for various radiotherapy clinical beams (Fix et al., 2004; Lewis et al., 1999) By simulating a large number

of particle histories, it was possible to achieve the particle fluence, energy spectrum, and dose distribution.

The percentage dose distribution of the absorbed dose in water and the beam profiles for various field sizes used clinically have been determined in this study. The Monte Carlo method of simulation completely depended on individual linear accelerator machine detail, machined geometry, the position of the materials, and the composition of each material.

2. MATERIALS AND METHODS

The linear accelerator head consisted of six component modules, including the target, the flattening filter, the ion chamber, the mirror, the field definition system (jaws and MLC's), and the reticle. The energy of the electrons were completely defined by a bending magnet, which then passed through the exit window and hit the target material. This generated high energy bremsstrahlung, which interacted with the electron beam. The beam profile below the target was like a Gaussian distribution which was flattened with the help of a flattening filter. Simulations were initiated with electrons striking the target. Primary and secondary particles were transported using a beam defining system. The flattening filter area at the top for the 6 and 15 MV were $\Pi (0.064) \text{ cm}^2$ and $\Pi (0.102) \text{ cm}^2$, respectively.

The intensity of the photons transported down was measured by a photon ion-chamber. This beam was further well-collimated by secondary collimators which moved in the x- and y-directions. Particles were transported to the plane above the secondary collimators, which was stored as a phase-space data file (PS file; Siebers et al., 1999) The phase-space data contained the necessary position, momentum, and energy of the traversing particle, which passed through the phase-space scoring plane.

The mirror generated the light field, which was required to adjust the patient positioning for the defined field by the jaw. The reticle was helpful in aligning the patient to the center of the field with the help of the lines drawn on it.

The mean energy of the electron incident on the target or exit window for the 6MV photon beam was 6MV and for the 15MV photon beam was 15 MV. The simulations were initiated with electron beams of a 1 mm radius incident on the target. All the particles produced, including the primary, were transported through the beam defining the geometry of the system like the primary collimator, vacuum window, flattening filter, monitor chamber, field light mirror, ion chamber, and secondary collimator, and then directed to the water phantom.

The phase-space file served as the source for the water phantom simulation keeping the water surface as $Z=0$. The general purpose Monte Carlo MCNP4C3 code was used in a model Clinac 2300 C/D linear accelerator to simulate 6 and 15MV photon beams with the proprietary data supplied by Varian Oncology Systems. The MCNP4C3 code was used for this purpose, which uses a class I algorithm for electron transport and knock-on electron generation, where loss to secondary electrons was accounted for by statistical sampling of an energy loss straggling distribution. Hence, the total collision stopping power values were used. It used the class II algorithm for bremsstrahlung production.

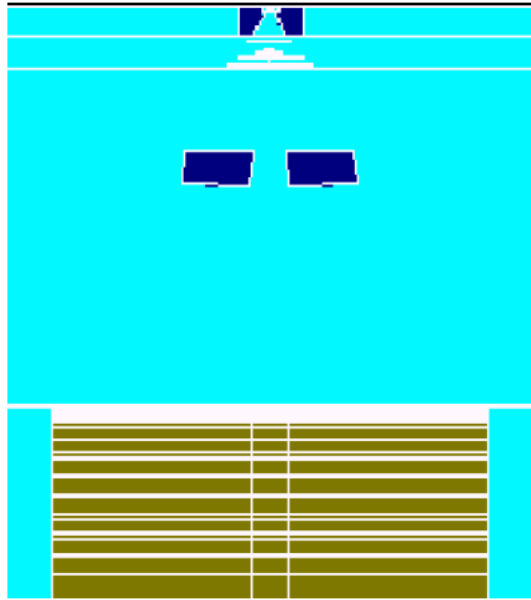


Fig 1. MCNP plot of the simulated part of the Clinac - 2300 C/D linear accelerator head and water phantom.

In the present work, out of the entire 24.5 cm radial field, the square fields ranging from 5 cm x 5 cm to 35 cm x 35 cm were taken in increments of 5cm, which were made by adjusting the secondary collimator jaws.

3. RESULTS AND DISCUSSION

The discrete threshold energies (ECUT and PCUT) for the creation of electrons and photons were set to 0.20 MeV and 0.01 MeV, respectively. When the particles reached these cut-off values, the energy was scored locally. The MCNP run used importance (IMP) and BREM bremsstrahlung splitting variance reduction cards.

The variance reduction technique was used for the cells to terminate the particle history if it was required for geometry splitting and Russian roulette to help the particles move to more sensitive regions of the geometry. The bremsstrahlung process generated many low-energy photons, but the higher energy photons were often of greater interest. The bremsstrahlung biasing was used to generate more high energy photons of interest, which contributed significantly to the energy absorption in the water phantom. The source specification card was used to describe various parameters of the radiation particle, such as the type of the radiation, its incident energy (15MeV), the radius of the particle beam (0.1 cm), the location of the particle incident on the target, the direction of the particle, and the surface where the source particle started. The F8 tally card was used to score the energy in various voxel cells which were arranged in the water phantom similar to the cells in the lattice structures.

The incident electron beam was assumed to be emerging from the 1 mm radius aperture perpendicular to the target before hitting it.

For cross-line profile studies, two different sizes of voxel cells were designed. The voxel cell size (0.6 cm x 4 cm x 1 cm) within the flattened region in the field sizes chosen were larger than the cell sizes (0.3 cm x 4 cm x 1 cm) in the penumbra region to determine the dose fall off points. Separate input files were prepared to generate the percentage depth dose data for different field sizes by keeping the voxel cells of size 4 cm x 4 cm x 1 cm along the central axis with a 1 cm interval gap, except in the build-up region.

In the simulation process, the particles were transported up to the phase space scoring plane just below the monitor chamber, but before the secondary collimators. Transport of the simulated particle was terminated when it left a predetermined exit of the scoring plane. The resulting particle coordinates, type, energy, position, and momentum were stored in the form of phase space distribution (PSD) file, which acted as a source of radiation for the second stage of simulation.

Towards the experimental beam data comparison, measurements were done using the radiation field analyzer (RFA-300 plus model), a 3D water phantom scanner with solid state detectors. The profiles were measured for the 6 and 15MV photon beams at a 100 cm SSD for field sizes 5 x 5 cm² to 35 x 35 cm² at various depths of Dmax, 5 cm, 10 cm, 15 cm, 20 cm, 25 cm, and 30 cm. The central axis depth dose data was measured for both 6 and 15MV photon beams. These measurements were done at 100 cm SSD for field sizes 5 x 5 cm², 10 x 10 cm², 15 x 15 cm², 20 x 20 cm², 25 x 25 cm², 30 x 30 cm², and 35 x 35 cm² using the RFA-300 plus system. These data were used for comparison and validation of the simulated data.

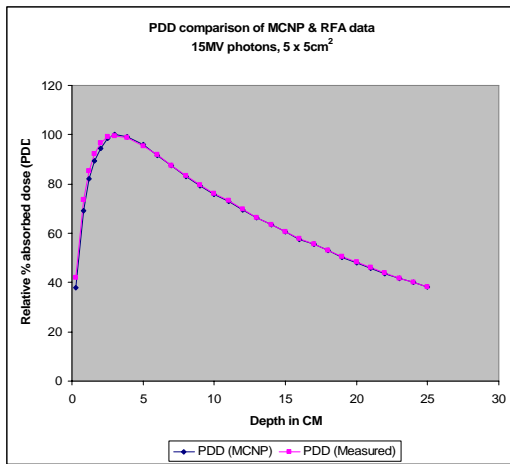


Fig. 2

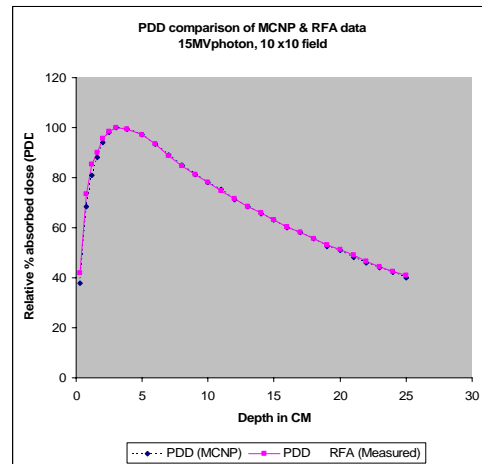


Fig. 3

Figures 2 & 3 compare the percentage depth dose data of the 15 MV photon MCNP simulated data for field sizes 5 x 5cm² and 10 x 10cm² with the measured RFA data. The values simulated with MCNP are within 2%, which is highly comparable with the RFA measurement.

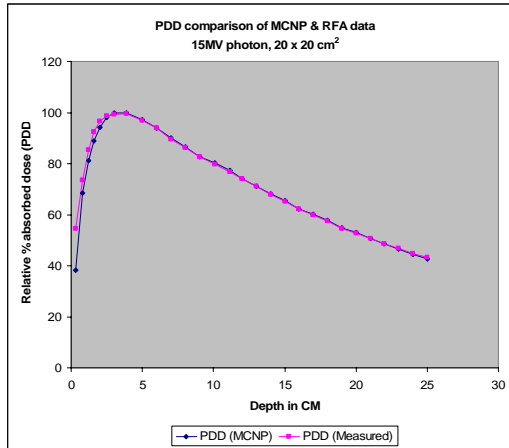


Fig. 4

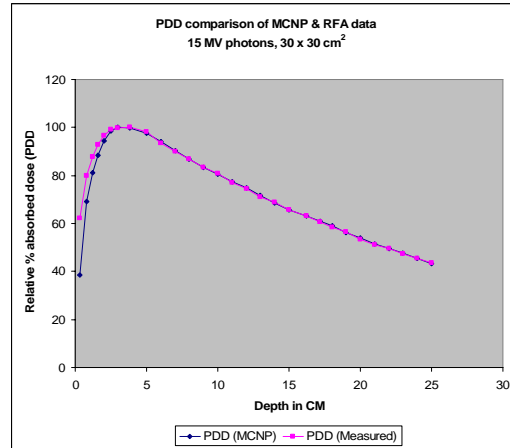


Fig.5

Figures 4 & 5 compare the percentage depth dose data of the 15MV photon MCNP simulated data for field sizes $20 \times 20 \text{ cm}^2$ and $30 \times 30 \text{ cm}^2$ with the measured RFA data. MCNP data appeared slightly high after the buildup region, which was due to the difference caused in the spatial resolution of the voxel size of simulation and could be improved, but within 2% beyond the buildup region.

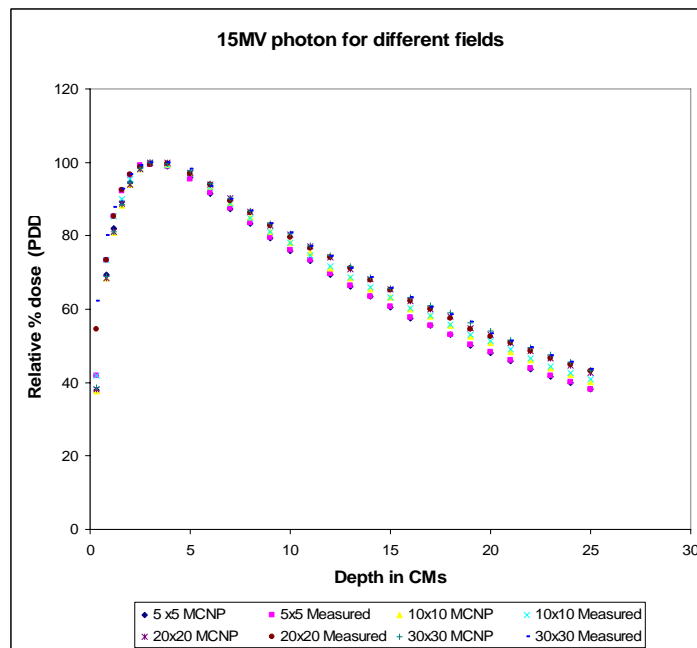


Fig. 6

Fig.6 Comparison of the PDDs of 15MV photons of measured (RFA) data with MCNP data for various field sizes of $5 \times 5 \text{ cm}^2$, $10 \times 10 \text{ cm}^2$, $20 \times 20 \text{ cm}^2$, and $30 \times 30 \text{ cm}^2$.

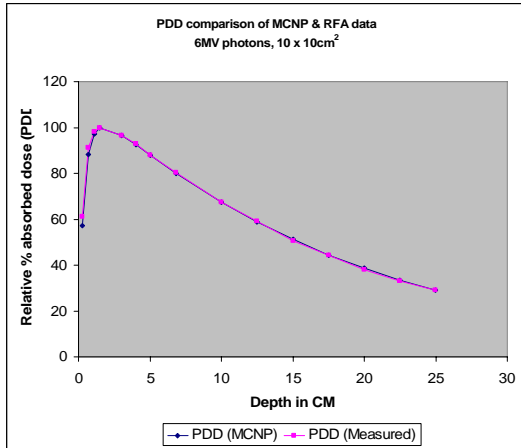


Fig. 7

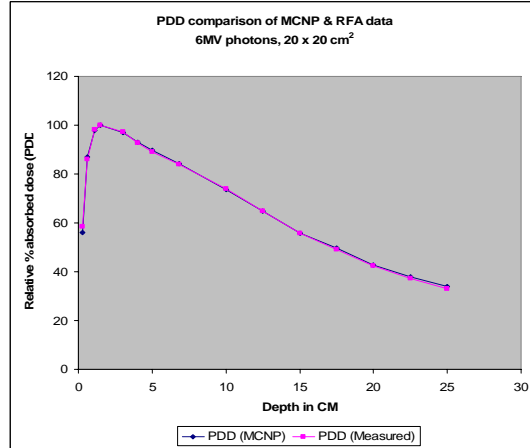


Fig.8

Figures 7 & 8 compare the percent depth dose curves of the Monte Carlo simulation for 6MV photons with the field sizes of $10 \times 10 \text{ cm}^2$ and $20 \times 20 \text{ cm}^2$ to measured RFA - data with a solid state detector. This showed a perfect increment in achieving the resolution, which was improved here to obtain a clear fit of the curve with the measured data in the buildup region, which was within 1%.

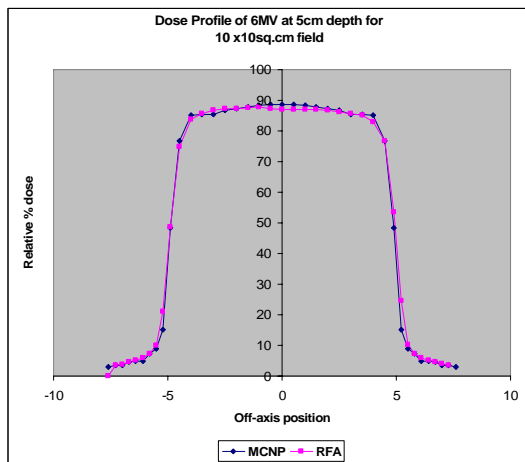


Fig.9

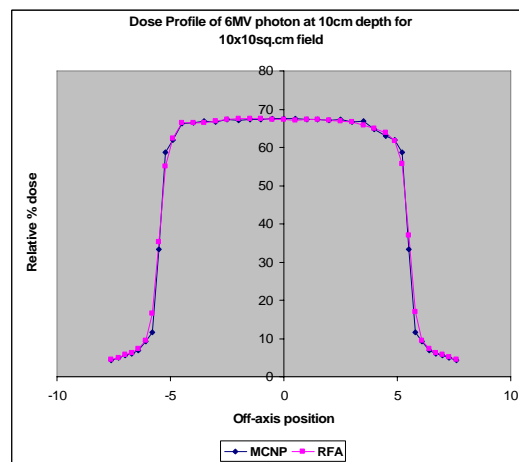


Fig.10

Figures 9 & 10 show the dose profiles of the 6MV photon comparison between the Monte Carlo simulation and the measured (RFA) data was within 1% at 100 cm SSD for the depths of 5 cm and 10 cm for a field size of $10 \times 10 \text{ cm}^2$.

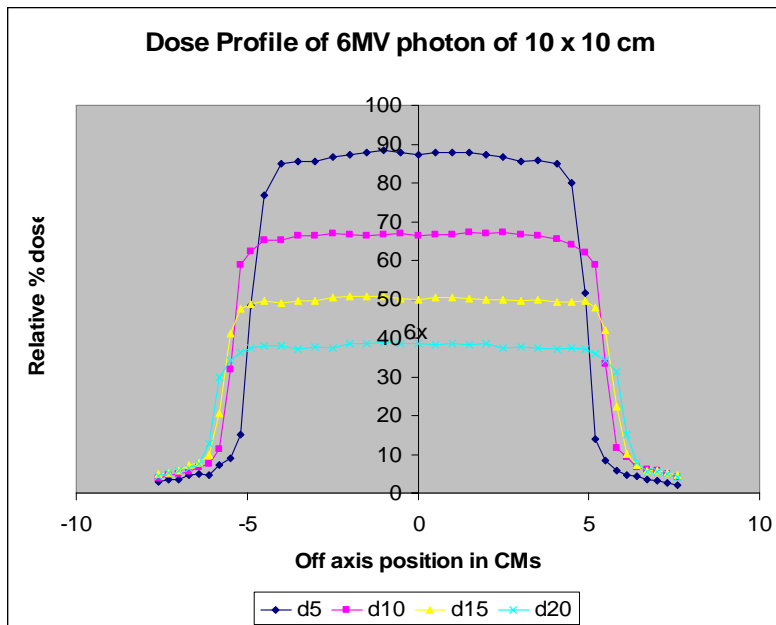


Fig.11

Figures 11 shows the dose profiles of the 6MV photon of the Monte Carlo simulation and the measured (RFA) data 100 cm SSD at depths of 5 cm, 10 cm, 15 cm, and 20 cm for a field size of $10 \times 10 \text{ cm}^2$.

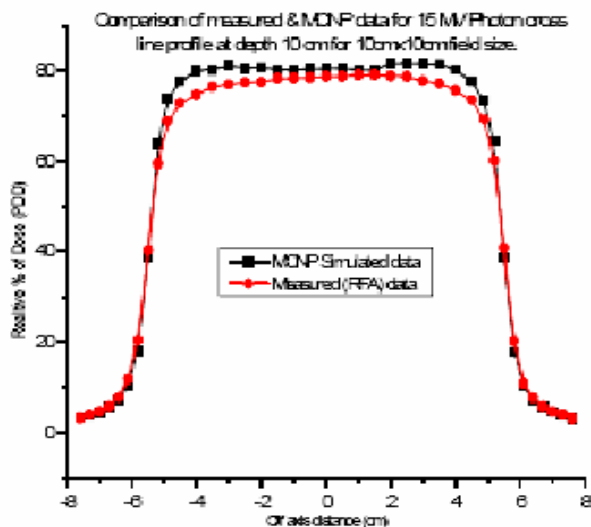


Fig.12

Figure 12 shows the dose profiles of the 15MV photon at a depth of 10 cm and SSD 100 cm for a field size $10 \times 10 \text{ cm}^2$. For the same depth, the electron and photon scattering angle increased when the energy decreased. This accounted for the increase in profile shoulders.

(Daryoush et. al., 2002). Also the profiles depicted the influence of spot size, which caused horn at the edge and brought down the width of the penumbra. (Lin et al., 2001).

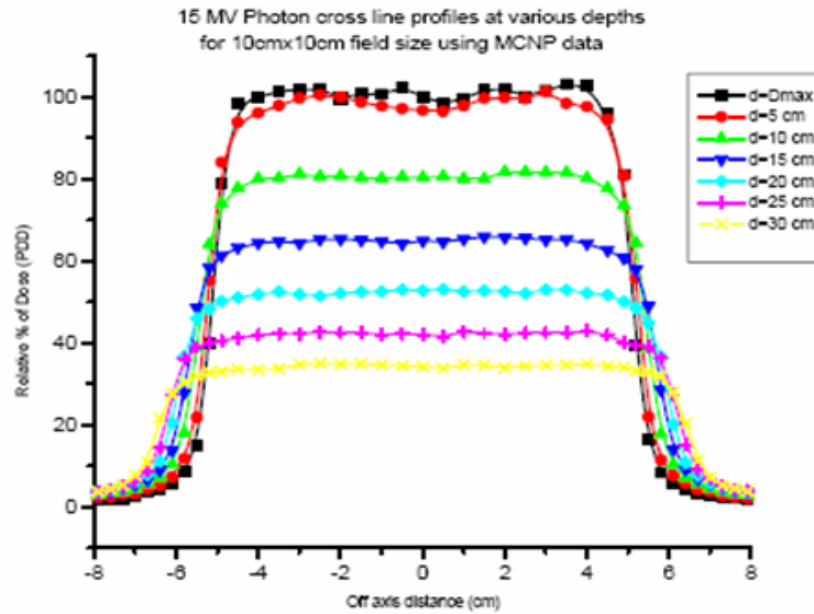


Fig .13

Figures 13 shows the dose profiles of the 15MV photon of the Monte Carlo simulation and the measured (RFA) data 100 cm SSD at depths of d_{max} , 5 cm, 10 cm, 15 cm, 20 cm, 25 cm, and 30 cm for a field size of $10 \times 10 \text{ cm}^2$.

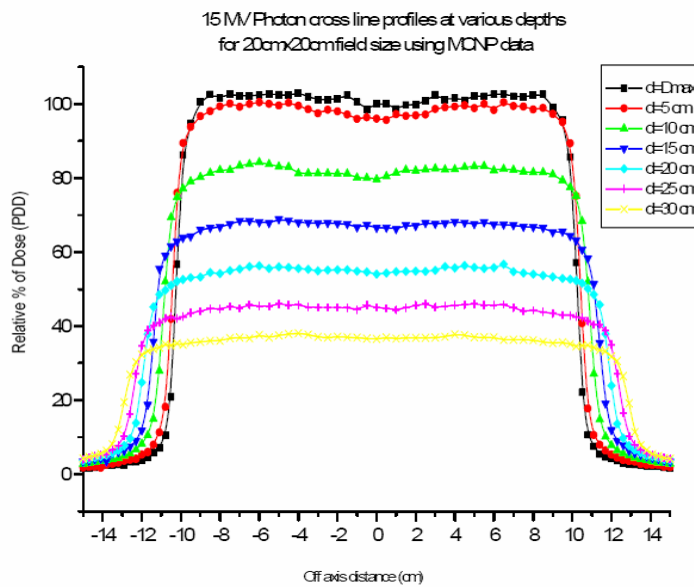


Fig. 14

Figure 14 shows the dose profiles of the 15MV photon of the Monte Carlo simulation and the measured (RFA) data 100 cm SSD at depths of d_{max} , 5 cm, 10 cm, 15 cm, 20 cm, 25 cm, and 30 cm for a field size of $20 \times 20 \text{ cm}^2$.

3. CONCLUSIONS

The average energy of the primary electron beam was 6 MeV for the 6 MV photons and 15 MeV for the 15 MV photons. The simulation of the Varian Linear Accelerator Clinac 2100C/D by the Monte Carlo code and validation was achieved. The results are encouraging through the comparison data and thus the IMRT phantom calculation data from the planning system was verified by simulation of this code. Further, in the complicated IMRT plans, the simulation or the validated data helped to know the exact dose to the vital organs which minimized the errors of measured data.

REFERENCES

1. Daryoush, S-B. and Rogers, D.W.O., *Sensitivity of mega voltage photon beam Monte Carlo simulation to electron beam and other parameters*, **Med. Phys** **29** (3), pp. 379–390, 2002.
2. Lin, SY., Chu, T.C., Lin, J.P., *Monte Carlo simulation of a clinical linear accelerator*. **Appl. Radiat. Isot.** **55** (6) pp.759-65, 2001.
3. Lovelock, D.M., Chui C.S. and Mohan, R., *A Monte Carlo model of photon beams used in radiation therapy*, **Med. Phys.**, **22**, pp.1387 – 1394, 1995.
4. Michael K. Fix, Paul J. Keall, Kathryn Dawson, and Jeffrey V. Siebers, *Monte Carlo source model for photon beam radiotherapy: Photon source characteristics*. **Med. Phys.** **31** (11), pp.3106-3121, 2004.
5. Rogers, D.W.O., *Fifty years of Monte Carlo simulation for medical physics*, **Phys. Med. Biol.**, **51**, pp. R287-R301. 2006
6. R.D. Lewis, S.J. Ryda, B.A. Hancock and C.J. Evans, *An MCNP based model of a linear accelerator*, **Phys. Med. Biol.**, **44**, pp.1219-1230, 1994.
7. Serrano, B., Hachen, A., Franchisseur, E., Herault, J., Marcie, S., Costa, A., Bensadoun, R.J., Barthe, J and Gerard, J.P., *Monte Carlo simulation of a medical linear accelerator for radiotherapy use*. **Radiation Protection Dosimetry**, **Vol. 119**, No.1-4, pp. 506-509, 2006
8. Verhaegen, F. and Seuntjens, J., *Monte Carlo modeling of external radiotherapy photon beams*. **Topical Rev. Phys. Med. Biol.** **48**, R107-R164, 2003.
9. Siebers, J., Libby, B. and Mohan, R., *Validation of Monte Carlo generated phase – space descriptions of medical linear accelerators*. **Med. Phys.** **26**, pp.1476-1483, 1999.
10. Ma C.M., Mok, E., Kapur, A., Pawlicki, T., Findley, D., Brain, S., Forster, K. and Boyer, A.L., *Clinical implementation of a Monte Carlo treatment planning system*. **Med Phys.** **26**, pp. 2133-2143, 1999.